

## Manifestation of coherent spin precession in stimulated semiconductor emission dynamics

S. Hallstein

*Max-Planck-Institut für Festkörperforschung, Heisenbergstraße 1, D-70569 Stuttgart, Germany*

J. D. Berger

*Optical Sciences Center, University of Arizona, Tucson, Arizona 85721*

M. Hilpert

*Max-Planck-Institut für Festkörperforschung, Heisenbergstraße 1, D-70569 Stuttgart, Germany*

H. C. Schneider, W. W. Rühle, F. Jahnke, and S. W. Koch

*Fachbereich Physik und Wissenschaftliches Zentrum für Materialwissenschaften der Philipps-Universität, Renthof 5, D-35032 Marburg, Germany*

H. M. Gibbs and G. Khitrova

*Optical Sciences Center, University of Arizona, Tucson, Arizona 85721*

M. Oestreich

*Fachbereich Physik und Wissenschaftliches Zentrum für Materialwissenschaften der Philipps-Universität, Renthof 5, D-35032 Marburg, Germany*

(Received 17 July 1997)

Circularly polarized optical excitation of a semiconductor microcavity in a transverse magnetic field leads to pulsed laser emission with alternating circular polarization synchronized to the electron Larmor precession. The synchronization originates from the transfer of electron-spin coherence to the dynamics of the optical field. A microscopic theory is developed to analyze the coupled carrier–light-field dynamics.

[S0163-1829(97)51636-5]

In this paper we show that the microscopic spin precession dynamics of semiconductor electrons in a magnetic field leads to real time modulations of a microcavity laser emission. Thus, a truly microscopic dynamical effect becomes macroscopically visible.

In our experiment we excite a semiconductor microcavity with circularly polarized light in Voigt geometry, where the magnetic field is applied perpendicular to both the quantum-well growth direction and the emission direction of the vertical cavity surface emitting laser (VCSEL). As an initial condition we create a spin-polarized electron distribution in the conduction band which then performs Larmor precessions around the magnetic field.<sup>1,2</sup> Under suitable conditions these coherent spin oscillations are transformed into a pulsing laser emission with a repetition rate determined by the electron Larmor frequency. To our knowledge, this is the first time that the interband emission of a semiconductor laser has been governed by electron spin dynamics.

For our experiments we use a semiconductor microcavity laser consisting of a  $3/2\lambda$  cavity with two 8 nm  $\text{In}_{0.04}\text{Ga}_{0.96}\text{As}$  quantum wells separated by GaAs barriers.<sup>3</sup> The wells are placed in the antinodes of the intracavity electric field, which is formed by two GaAs/AlAs distributed Bragg reflectors with 99.6% reflectivities. The sample is held at a temperature of 15 K in a 16 T superconducting magnet. The microcavity is excited with circularly polarized pulses of a Ti:sapphire laser with a 2 ps pulse length, 80 MHz repetition rate, and 780 nm wavelength. The pump wavelength is

above the microcavity stop band, so that both the quantum wells and the barriers are excited.

Choosing the  $z$  axis of our coordinate system in the growth direction, we align the magnetic field in the plane of the wells, i.e., in the  $x$  direction (Voigt geometry). The microcavity emission at 835 nm is detected in reflection geometry along the  $z$  axis, spectrally dispersed in a 0.32 m spectrometer, and temporally resolved in a synchroscan streak camera with a time resolution of 7 ps (full width at half maximum of the exciting laser pulse).

In Fig. 1(a) we show the time-resolved laser emission of our VCSEL for an excitation power of 35 mW and a magnetic-field strength of 2 T. Pulsed laser emission with a modulation depth of approximately 96% is clearly seen. The pulse repetition rate is 22 GHz, corresponding to twice the electron Larmor frequency of our system. For comparison, we show in Fig. 1(b) the emission of a quantum-well reference sample without a cavity. Under otherwise identical excitation conditions, there are *no* oscillations present.

In order to analyze the transfer of the coherent spin dynamics to the microcavity laser emission, we have developed a microscopic theory. For the analysis of optical experiments it is conventional and most convenient to choose the growth direction as quantization direction for momentum, angular momentum, spin, etc.<sup>4</sup> Hence, the applied magnetic field in Voigt geometry does not lead to a splitting of the spin degenerate bands as would be the case for a quantization in the  $B$ -field direction  $z$ . But, as a consequence of the applied

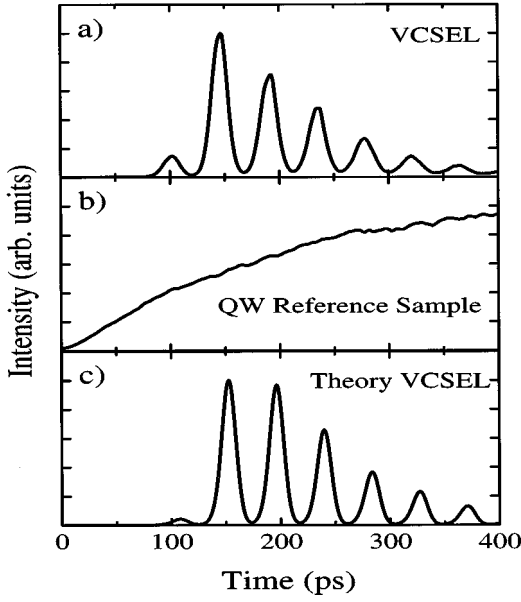


FIG. 1. (a) Time-resolved stimulated emission of the quantum-well microcavity laser in a 2 T magnetic field. (b) Time-resolved emission of the quantum-well reference sample without a cavity. (c) Computed microcavity emission with parameters corresponding to the conditions of (a).

magnetic field, we have a coherent coupling between the conduction band states with opposite spins via the “Larmor polarization” in much the same way as the optical interband polarization couples conduction and valence bands in the semiconductor Bloch equations.<sup>4</sup> The holes do not contribute to the  $B$ -field-dependent dynamics since the expectation value of the heavy-hole angular momentum in the observation direction vanishes in this geometry.<sup>5</sup>

The temporal development of the total electron spin-up and spin-down components is determined by the dynamics of the respective electron distributions. Our model calculations assume that the circularly polarized laser excitation leads to a preferential electron-spin orientation (in the  $z$  direction) since the optical transition probabilities for the heavy-hole and light-hole transitions are different. The magnetic dipole interaction between the electron magnetic moment in the  $z$  direction and the applied magnetic field in the  $x$  direction causes electronic Larmor oscillations with the frequency  $\omega_L = g_e \mu_B B / \hbar$ . Here,  $g_e$  is the electron Landé  $g$  factor.

To compute the VCSEL emission dynamics we need the temporal evolution of the electron distributions in the spin-split bands. Hence, we use a nonequilibrium theory in a simple two-band model, which includes the coupling of the parabolic electron and hole bands via the dipole interaction. The projection of the total angular momentum on the  $z$  axis can assume the values  $m_s = \pm 1/2$  for the electron bands which will be denoted by the subscripts “+” and “-.” Consequently, our dynamical variables are the electron distribution functions  $f_{\pm}^e$  and the Larmor polarization between the electron bands, defined by  $\psi(k) = \langle a_+^{\dagger}(k) a_-(k) \rangle$ . Here  $\langle \dots \rangle$  denotes a quantum statistical average and  $a_{\pm}(k)$  is the destruction operator for an electron with crystal momentum  $k$  and magnetic quantum number  $m_s = \pm 1/2$ .

In a fashion analogous to the derivation of the semiconductor Bloch equations (SBE),<sup>4</sup> we obtain screened Hartree-Fock equations of motion

$$\left. \frac{\partial f_{\pm}^e(\mathbf{k})}{\partial t} \right|_B = 2 \text{Im}[\Omega_L^*(\mathbf{k}) \psi(\mathbf{k})], \quad (1)$$

with the renormalized Larmor frequency  $\hbar \Omega_L(\mathbf{k}) = \omega_L/2 - \sum_{\mathbf{k}'} V_{\mathbf{k},\mathbf{k}'} \psi(\mathbf{k}')$ , where  $V$  is the Coulomb potential. For the Larmor polarization we have

$$i \frac{\partial \psi(\mathbf{k})}{\partial t} = \omega^e \psi(\mathbf{k}) - \Omega_L(\mathbf{k}) [f_-^e(\mathbf{k}) - f_+^e(\mathbf{k})], \quad (2)$$

where the free polarization rotation is due to the Coulomb interaction  $\hbar \omega^e = - \sum_{\mathbf{k}'} V_{\mathbf{k},\mathbf{k}'} [f_-^e(\mathbf{k}') - f_+^e(\mathbf{k}')]$ . The fast relaxation of hole spins and the thermalization of electrons and holes are taken into account in a  $k$ -dependent rate-equation approximation. We use a single plasmon-pole approximation for the plasma screening at high densities. The microcavity laser is modeled by rate equations for the emission intensity. The gain is computed from the nonequilibrium distribution functions by using a matrix inversion technique.<sup>4</sup> Using material and excitation parameters typical for the experimental system,<sup>6</sup> we obtain the time-resolved laser emission curves.

The theoretical results for the conditions of Fig. 1(a) are presented in Fig. 1(c). The comparison between theory and experiment shows good overall agreement. The observed laser oscillation dynamics can be traced back to the dynamics of the two different carrier distribution functions for spin-up and spin-down electrons, which are originally generated by the circularly polarized high excitation of the sample in the presence of a magnetic field in Voigt geometry. The respective spin-up and spin-down carrier distributions lead to a time-dependent absorption (gain) for the circularly polarized  $\sigma^+$  (electron spin-down) and  $\sigma^-$  (electron spin-up) light emission components. For the experimental conditions reported here, it turns out that after the original excitation, first the gain for  $\sigma^-$  polarized light exceeds the losses at the emission energy and the  $\sigma^-$  emission is therefore strongly amplified. Emission of  $\sigma^+$  light, at this time, should therefore only be of a spontaneous nature. After a quarter precession period ( $t = T_L/4$ ), a sufficient amount of carriers have been transferred to the spin-down band, such that the gain for both light polarizations drops below threshold. Hence, lasing is switched off and the total microcavity emission reaches a minimum. After half a Larmor precession period ( $t = T_L/2$ ), the laser exceeds threshold again, this time, however, for  $\sigma^+$  light. The computed results for the two circular polarization components are shown in Figs. 2(a) and 2(c), respectively. The corresponding experimental curves in Figs. 2(b) and 2(d), obtained from the emission in Fig. 1(a) with the help of a circular analyzer, nicely confirm the theoretical results.

Hence, the total laser emission pulses with twice the Larmor frequency and alternating circular polarization. The Larmor frequency depends only on the magnetic field and the electron  $g$  factor. For the latter we deduce, with a 2 T magnetic field and a 22 GHz modulation frequency of the total emission, a value of  $g_e = -0.411$ , which is close to the electron  $g$  factor of bulk GaAs.<sup>2</sup> This is expected for our system.

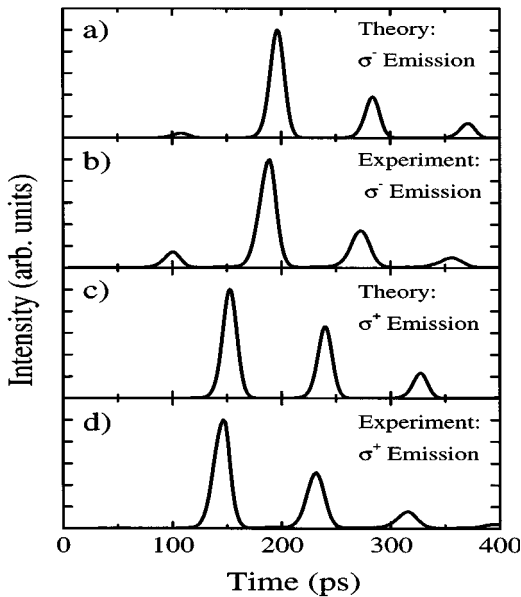


FIG. 2. Circularly polarized components of the microcavity emission of Fig. 1. The computed (measured) results for  $\sigma^-$  are shown in (a) and (b), and those for  $\sigma^+$  in (c) and (d), respectively.

Besides the synchronization of the stimulated emission to the electron Larmor precession, the presented experiment is a tool to transfer spin coherence to the stimulated oscillation dynamics of an optical field. We demonstrate pulse repetition rates of 22 GHz with a modulation depth of 96% in the total laser emission, and a modulation depth larger than 99% in the circularly polarized laser emission. A reduction of the modulation depth to 60% in 44 GHz oscillations of the total emission measured at a magnetic field of 4 T indicates a high-frequency limit imposed by the emission dynamics of our microcavity. Faster oscillations at higher magnetic fields or in materials with a larger  $g$  factor are possible,<sup>7</sup> but require a faster rise and decay time of the stimulated microcavity emission.

The modulation depth in the total emission strongly depends on the excitation power, since the oscillations arise from a modulation of the optical gain. Figure 3 demonstrates the influence of excitation power on the total microcavity laser emission. For low excitation power the laser remains below threshold at all times and no modulation is observed. Higher excitation leads to an increased maximum gain for  $\sigma^+$  and  $\sigma^-$  light, and to a larger stimulated part in the total emission. Oscillations begin to appear on top of a spontaneous emission background. The modulation depth grows with increasing excitation, due to the growing relative strength of the stimulated emission. A modulation depth of 96% is reached at an excitation power of 35 mW. For an even higher excitation, the modulation depth decreases again, indicating incomplete switch-off of the total laser emission between

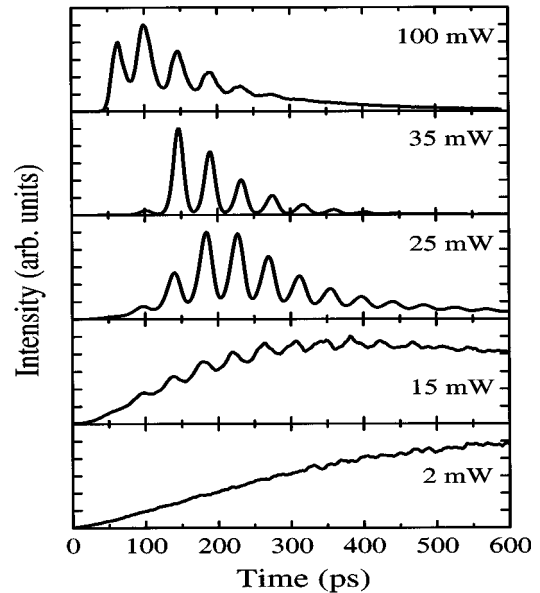


FIG. 3. Time-resolved total laser emission for increasing excitation powers at a magnetic field of 2 T.

consecutive pulses. In this high excitation regime, nonequilibrium carrier effects become important, which are under current investigation.

In conclusion, our investigations show that it is possible to transfer the coherent Larmor precession of semiconductor electron spins to the optical field emitted from a microcavity laser. We observe pulsed microcavity laser emission with twice the Larmor frequency and alternating circular polarization. Even though these experiments do not crucially depend on the strong light-matter coupling which can be realized in microcavities, the VCSEL geometry is necessary to realize the Voigt geometry and to create an electron-spin polarization based on the optical selection rules and transition probabilities. Furthermore, the tunable single longitudinal mode VCSEL emission characteristics allow us to observe the spin oscillations very clearly. A microscopic model for the spin-split states in the framework of semiconductor Bloch equations has been developed to analyze the data. The theory indicates the possibility of interesting nonequilibrium many-body effects in the spin-precession clock system.

The authors would like to thank H. J. Queisser and H. Giessen for helpful discussions, R. A. Wyss for critical reading of the manuscript, H. Klann and K. Rother for technical assistance, and the Forschungszentrum Jülich for a grant for CPU time. The work has been partially supported by the Schwerpunkt ‘‘Quantenkohärenz in Halbleitern’’ of the Deutsche Forschungsgemeinschaft, by the Leibniz prize, and by NSF Atomic, Molecular, and Optical Physics and Light-wave Technology and DARPA/ARO Ultraphotonics.

<sup>1</sup>A. P. Heberle, W. W. Rühle, and K. Ploog, *Phys. Rev. Lett.* **72**, 3887 (1994).

<sup>2</sup>M. Oestreich and W. W. Rühle, *Phys. Rev. Lett.* **74**, 2315 (1995); M. Oestreich *et al.*, *Phys. Rev. B* **53**, 7911 (1996); R. M. Han-nak *et al.*, *Solid State Commun.* **93**, 313 (1995).

<sup>3</sup>J. D. Berger *et al.*, *Phys. Rev. B* **54**, 1975 (1996); C. Weisbuch, M. Nishioka, A. Ishikawa, and Y. Arakawa, *Phys. Rev. Lett.* **69**, 3314 (1992).

<sup>4</sup>For a textbook discussion, see H. Haug and S. W. Koch, *Quantum Theory of the Optical and Electronic Properties of Semiconduc-*

- tors*, 3rd ed. (World Scientific, Singapore, 1994).
- <sup>5</sup>S. Bar-Ad and I. Bar-Joseph, *Phys. Rev. Lett.* **66**, 2491 (1991).
- <sup>6</sup>The material parameters used in the calculations are cavity-damping time 2 ps,  $m_e=0.0665m_0$ ,  $m_h=0.234m_0$ , carrier-carrier scattering rate 100 fs, thermalization rate 30 ps, hole-spin relaxation rate 5 ps, electron-spin relaxation rate 500 ps, spontaneous emission rate 800 ps and coupling  $10^{-3}$ , transverse mode overlap 0.2, pump field polarization 0.5, and Rabi energy  $1.6E_B$ .
- <sup>7</sup>S. A. Crooker, J. J. Baumberg, F. Flack, N. Samarth, and D. D. Awschalom, *Phys. Rev. Lett.* **77**, 2814 (1996).